Near-room-temperature control of magnetization in field effect devices based on La 0.67 Sr 0.33 MnO 3 thin films

S. Brivio, M. Cantoni, D. Petti, and R. Bertacco

Citation: Journal of Applied Physics **108**, 113906 (2010); doi: 10.1063/1.3516283
View online: http://dx.doi.org/10.1063/1.3516283
View Table of Contents: http://scitation.aip.org/content/aip/journal/jap/108/11?ver=pdfcov
Published by the AIP Publishing

Near-room-temperature control of magnetization in field effect devices based on $La_{0.67}Sr_{0.33}MnO_3$ thin films

S. Brivio,[a] M. Cantoni, D. Petti, and R. Bertacco
Dipartimento di Fisica, L-NESS and CNISM, Politecnico di Milano, via Anzani 42, 22100 Como, Italy

(Received 2 July 2010; accepted 16 October 2010; published online 3 December 2010)

The control of the magnetization in ferromagnetic layers via electric fields is a hot topic in view of applications to the next generation of spintronic devices, where writing the magnetic information through current lines could be replaced by electric writing. Mixed valence manganites are good candidates for such a purpose because they present an intriguing coupling between ferromagnetism and charge ordering/doping which can be tuned by the application of an electric field. Here we present results on the near-room temperature control of the magnetization of optimally doped $La_{0.67}Sr_{0.33}MnO_3$ ultrathin films in vertical field effect devices, where they act as top or bottom electrodes. In the latter case a slight decrease in the Curie temperature (~5 K) is observed after application of 5×10^7 V/m, i.e., the maximum field preventing electric breakdown, compatible with the induced variation in the charge density and mixed valence within the Thomas Fermi screening length. These results indicate that electric fields achievable in vertical field effect devices, of the same entity of interfacial fields originating from differences in the work function in heterostructures, have only minor influence on the magnetic properties of optimally doped ultrathin $La_{0.67}Sr_{0.33}MnO_3$ films. © *2010 American Institute of Physics*. [doi:10.1063/1.3516283]

I. INTRODUCTION

The possibility of achieving the electric control of the magnetization in a ferromagnetic material has attracted a huge interest in the past years, especially in view of applications to spintronic devices where the information is stored in the magnetic state of a ferromagnetic electrode. Changing the writing strategy, from the one employing current lines to a new one, where a pure electric field causes a sizable change in the magnetization, would represent a true breakthrough. In fact writing a magnetic information in a ferromagnetic electrode via a magnetic field produced by current lines is an inefficient process at least for two reasons: (i) it implies energy dissipation related to Joule effect; (ii) the technology is not scalable because it is difficult to confine magnetic fields at the nanoscale, so that obtaining high densities of devices is a great challenge. On the contrary the totally electric writing and reading of magnetically stored information would represent a significant advance toward devices like nonvolatile magnetic random access memories combining fast access, scalability, and the intrinsic high stability of magnetic devices. In principle bulk multiferroic materials, displaying intrinsic magnetoelectric coupling, would be the ideal solution (for a review see Ref. 1). However, the lack of robust multiferroic materials operating near room temperature (RT)[2] leads to the investigation of other possible solutions typically involving interfaces or ultrathin films.

In this scenario mixed valence manganites in the form $Re_{1-x}M_xMnO_3$ (where Re is a rare earth element, like La or Nd, and M is a divalent metal, like Sr or Ca) have received a renewed attention: as a matter of fact, their intrinsic sensitivity to external perturbations is very appealing in view of novel devices, in which the ferromagnetic properties could be modulated by electric fields, strain, light, etc.[3] In fact in manganites the ferromagnetic coupling is weaker than in the standard 3d ferromagnets, so that the electric control of their magnetization is in principle easier than in conventional magnetic materials. Furthermore, the limited carrier concentration (10^{21}–10^{22} cm^{-3}) implies a higher screening length in manganites with respect to standard metals, thus increasing the penetration depth of electric fields. Finally the peculiar cross-couplings between ferromagnetism and strain/charge concentration play a major role in the physics of manganites, so that many different approaches can be followed in order to influence the magnetization without external magnetic fields. The electric control of manganite magnetization can be achieved through different kinds of interactions. Eerenstein *et al.*[4] reported a large magnetoelectric coupling in the structure composed of a 50 nm thick $La_{0.67}Sr_{0.33}MnO_3$ (LSMO) film grown on top of a piezoelectric $BaTiO_3$ single crystal, essentially due to tuning of the Jahn–Teller effect[5] via controlled strain, thus altering the ferromagnetic character.[6,7] On the other hand, charge injection can effectively modify the relative concentration of Mn^{3+} and Mn^{4+} ions and, hence, lead to a sizable variation in the ferromagnetic moment and exchange energy as well.[8] Molegraaf *et al.*[9] succeeded in inducing charge accumulation in a 4 nm thick LSMO film by exploiting the high polarization of a ferroelectric $PbZr_{0.2}Ti_{0.8}O_3$ top layer and measured both magnetization (up to ~15% at 100 K) and Curie temperature (~20 K) variations. However none of these papers reports on sizable effects at RT, suitable for practical applications.

In this paper, we report on the influence of electric fields on the near RT Curie temperature (T_C) of LSMO ultrathin films embedded in vertical field effect devices (FEDs), allowing to control the amount of charge injected in a thin interfacial layer of LSMO, in the order of the screening

[a]Author to whom correspondence should be sent. Electronic mail: stefano3.brivio@como.polimi.it.

length (roughly 0.2 nm).[10] The electric field was applied to the LSMO layer through an insulating $SrTiO_3$ (STO) barrier, as in a standard FED, where LSMO plays the role of the active material. The use of a high-k insulator such as STO assures a high charge injection efficiency for a given applied voltage. Two different FED vertical structures have been tested: (i) Au/STO/LSMO (top-gated) and (ii) LSMO/STO/Nb-doped STO (back-gated), in which the electric field acts, across the STO film, on the top and on the bottom of the LSMO layer, respectively. Note that similar structures were produced and analyzed by Pallecchi *et al.*[11] in a lateral geometry. The application of an electric field to their structures produced a change in LSMO resistivity up to 250% at low temperatures and a shift of 43 K of the metal insulator transition temperature. However, also in this case field effects were detected only at low temperature, i.e., in a range not suitable for practical applications.

On the contrary our work was focused on magnetoelectric effects near RT, and to this scope ultrathin films of the optimally doped manganite LSMO, with T_C close to RT, have been investigated. In our vertical FED structures we observed a small T_C variation (~5 K) near RT upon electric field application in structure (i): Au/STO/LSMO (top-gated). We found a good agreement between the observed shift in T_C and the expected shift on the basis of the interfacial alteration of the manganite doping estimated from the injected charge. These results indicate that only minor magnetoelectric effects can be achieved in practical devices based on optimally doped manganites operating at RT, while higher effects, like the huge decrease of T_C in ultrathin films of LSMO when capped with Au nanoparticles reported by our group[12–14] are not due to electrostatic effects.

II. EXPERIMENT

Perovskite based field effect heterostructures have been prepared by pulsed laser deposition (PLD) and molecular beam epitaxy (MBE) in the apparatus described in Ref. 15. LSMO and STO deposition conditions were optimized in order to achieve good epitaxy and low surface roughness. STO substrates were annealed at 1000 K for 10 min in oxygen flux, at a pressure of 30 Pa; the same temperature and oxygen pressure were kept during the PLD deposition. A Q-switched frequency quadrupled Nd:YAG laser (wavelength 266 nm) was used, providing a fluence of 3 J/cm^2 at a repetition rate of 2 Hz. The target-substrate distance was set to 37.5 mm. The growth of LSMO and STO layers was monitored by *in situ* real-time reflection high energy electron diffraction (RHEED). After deposition, the samples were annealed at 673 K for 15 min in 1 atm of pure oxygen in order to fill oxygen vacancies. LSMO films grown with this procedure were characterized by x-ray diffraction (XRD) with a commercial Bruker D8 Advance diffractometer equipped with a 4-circle goniometer and area detector.

Two kinds of heterostructures and corresponding devices have been fabricated, as shown in Fig. 1: (i) *back-gated FEDs* [Fig. 1(a)] where the bottom electrode is a 1 wt % Nb doped STO (Nb:STO) substrate with (001) orientation, on top of which the STO barrier and thin LSMO films (3 and 4 nm thick) were epitaxially grown by PLD; (ii) *top-gated FEDs* [Fig. 1(b)] where a 4 nm LSMO film, grown on an undoped STO substrate with (001) orientation, acts as bottom electrode buried under an epitaxial STO barrier, while the top electrode is a Au overlayer grown by MBE. LSMO films thinner than 4 nm have not been considered in top-gated FEDs because the light attenuation due to the top Au gate during magneto-optical characterization produced an unacceptable signal-to-noise ratio. Heterostructures have been completely grown *in situ*, in order to avoid any contamination at the interfaces.

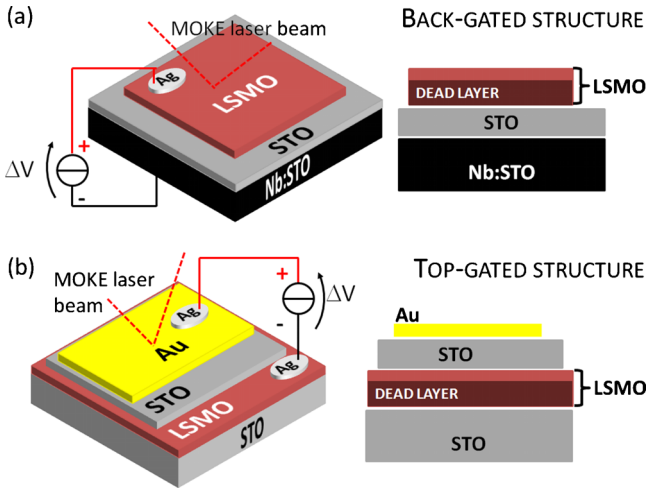

FIG. 1. (Color online) Sketch and lateral view of back-gated FEDs (panel a), and top-gated FEDs (panel b). The laser beam path illustrates the geometry used in MOKE experiments. In the lateral view the location of the LSMO dead layer is indicated.

The magnetoelectric characterization was performed by magneto-optic Kerr effect (MOKE), recording the Kerr ellipticity in longitudinal configuration with a photoelastic modulator (PEM), under different bias conditions. The light was produced by a stabilized 638 nm DC laser diode. To overcome the inherent experimental difficulties related to the low signal arising from ultrathin LSMO films, a double lock-in technique has been employed, including modulation of the external magnetic field at a frequency of 61 Hz. The signal from the photodiode was demodulated, with a first lock-in, at the frequency (50 KHz) of the PEM and then at 61 Hz with a second lock-in. In this way, the amplitude of the magneto-optical hysteresis loop, proportional to the magnetization, has been recorded as a function of temperature and applied electric field, as described also by Molegraaf *et al.*[9]

During the MOKE measurements, voltages were applied between top and bottom electrodes with a Keithley 2601, while keeping the bottom electrode connected to the ground. The samples were lodged in a closed circuit He cryostat allowing for measurements at different temperatures.

III. RESULTS

Figure 2(a) shows the high quality of epitaxial growth by PLD: the oscillations of the RHEED intensity recorded during deposition of LSMO (top curve, blue online) and STO (bottom curve, red online) indicate a layer-by-layer growth evolving toward a step flow growth mode. From the RHEED

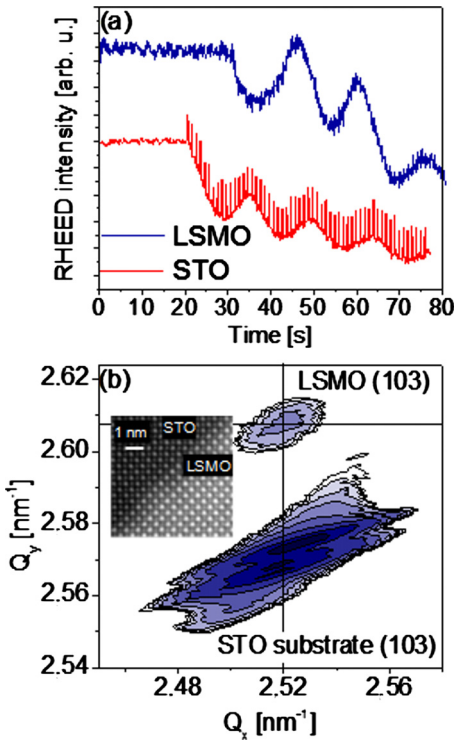

FIG. 2. (Color online) (a) RHEED oscillations recorded during the PLD growth of LSMO (blue top curve) and STO (red bottom curve); (b) Q-plot of a LSMO//STO film around the (103) reflection. In the inset of panel (b) a dark field transmission electron microscopy image of a STO/LSMO interface between a STO film grown on an LSMO thin film is shown.

oscillations the deposition rate was precisely determined to be 0.014 nm/pulse for STO and 0.012 nm/pulse for LSMO. In Fig. 2(b) a q-plot around the (103) reflection of a 34 nm thick LSMO film, grown in such optimal conditions on a STO substrate, is shown. The Q-plot reveals the coherent growth of LSMO on STO: indeed almost perfect matching of the in-plane parameter is achieved between the LSMO overlayer and the STO substrate. The LSMO lattice parameters are 0.390 nm in plane and 0.385 nm out of plane. Interfaces are atomically sharp, as clearly seen from the dark field scanning transmission electron microscopy (STEM) (Ref. 16) image in the inset of Fig. 2(b) showing in detail the LSMO/STO interface.

Due to the limited extent of the region affected by the electric field in LSMO (the Thomas Fermi screening length for LSMO is $\lambda_{LSMO} \sim 0.2$ nm), very thin manganite films are needed for observing sizable variations in FEDs. In addition we must take into account the formation of the so called "dead layer" at the interface between manganite films and substrates,[10,17,18] determined to be in the order of 3 nm in our films by resistivity and nuclear magnetic resonance measurements,[12,14] which further reduces the thickness of the film with nominal magnetic properties. According to these constraints, we analyzed FEDs with LSMO thickness between 2 and 4 nm, in order to find for each configuration the minimum thickness giving a reasonable MOKE signal to be monitored as a function of the applied electric field. Incidentally, we found that 2 nm of LSMO are not magnetic, within the sensitivity of our MOKE apparatus described above, while 3 nm give a reasonable MOKE signal only if they are directly exposed to the laser beam. This indicates that the extension of the dead layer is in between 2 and 3 nm while the optimum LSMO thickness for top-gated and back-gated FEDs are 4 nm and 3 nm respectively, as in the devices investigated in the present paper. In a previous paper,[12] we demonstrated that films in this thickness range are conductive and can be fruitfully employed as electrodes. In order to reduce the contact resistance between the electrodes and the voltage probes, small pads of Ag have been deposited by electron beam evaporation on top of the Au and LSMO electrodes.

Different thicknesses of the STO barrier were tested. When a dc voltage (in the order of a few Volts) is applied between the electrodes, the leakage current between top and bottom electrode must be as low as possible in order to prevent spurious heating effects and nonuniform distributions of the electric potential arising from local shorts. In particular in the top-gated configuration, the presence of some droplets on the surface of the LSMO layer, with typical height in the range of tens of nanometers and density lower than 4×10^{-4} μm^{-2}, can facilitate the creation of conductive paths through the STO barrier. Also in structures with relatively large STO thickness (100 nm) and reduced leakage (less than 10 nA/mm^2 for an applied voltage of 5 V) the dielectric breakdown of the STO barrier limits the lifetime of the devices due to progressive opening of conductive channels in correspondence of droplets and defects, possibly via electromigration.[19] As a compromise between the requirement of low leakage currents and the aim of achieving high fields while applying low voltages, compatible with standard complementary metal-oxide semiconductor electronics, in this paper we report data on FEDs with a STO thickness of 50–100 nm. In this way the leakage current was always ≤ 10 nA, low enough to exclude any Joule heating effect on the LSMO layer.

In the top-gated structure different thicknesses of the top Au layer have been tested and finally 6 nm was chosen, as it guarantees electrical continuity together with low light attenuation in MOKE experiments. The results of magnetoelectric measurements in the case of the back-gated structure are summarized in Fig. 3(a). The LSMO and STO thicknesses are, respectively, 3 nm and 100 nm. The Kerr amplitude is displayed as a function of the sample temperature for different bias voltages (ΔV) between LSMO and the conductive substrate. As expected, the Kerr amplitude drops to zero at a particular temperature, which indicates the Curie Temperature (T_C). For zero bias (middle curve) we obtained $T_C = 286 \pm 2$ K, as estimated with the graphical method shown in Fig. 3. This value is lower than the bulk value (around 350 K) but very close to RT, as expected for high quality ultrathin films of optimally doped LSMO.[18] The application of $\Delta V = \pm 10$ V does not produce any sizable variation in T_C within the experimental accuracy. Very similar results were obtained also for a 4 nm thick LSMO film in a back-gated FED (data not shown): T_C is slightly higher (294 ± 2 K), as expected for a thicker film, but insensitive to the applied voltage.

Figure 3(b) shows similar measurements performed on a top-gated structure: Au(6 nm)/STO(50 nm)/LSMO(4 nm).

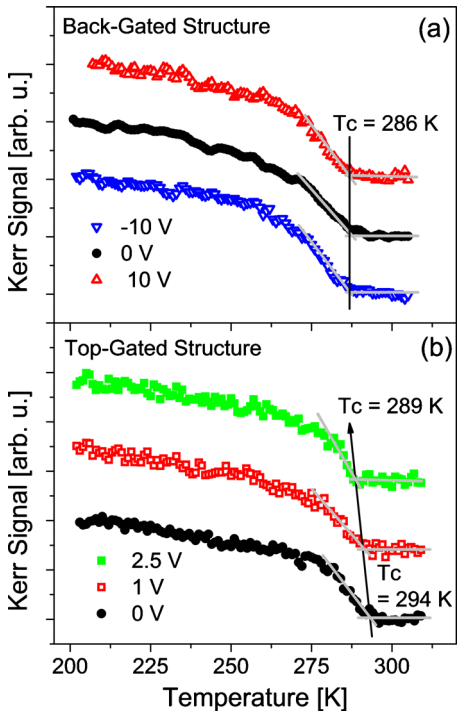

FIG. 3. (Color online) (a) Kerr signal from a 3 nm LSMO film in the back-gated structure at different applied voltages (−10 V—blue down triangles, 0 V—black filled dots, 10 V—red up triangles). No change in the Curie temperature is detected in this case. (b) Kerr signal from a 4 nm LSMO film in the top-gated structure at different applied voltages (0 V—black filled dots, 1 V—red empty squares, 2.5 V—green filled squares). A progressive decrease in the Curie temperature is detected, with a maximum variation of 5 K.

The Kerr amplitude as a function of temperature is reported for three different bias voltages: 0, 1, and 2.5 V. With zero bias (bottom curve, black online) $T_C = 294 \pm 2$ K, while the application of bias causes a progressive decrease in T_C with a maximum variation of 5 K for a positive bias of 2.5 V. The application of a higher electric field led to the electric breakdown of the barrier.

IV. DISCUSSION

The main difference between the two structures investigated lies in the side where the penetration of the electric field through the LSMO film occurs. In the back-gated structure the electric field is applied from the bottom, whereas in the top-gated structure the field is applied from the top, as can be appreciated in the lateral views of Fig. 1. This is not a merely geometrical difference, by virtue of the intrinsic vertical inhomogeneity of thin manganite films related to the formation of a dead layer, 2–3 nm thick, at the interface with oxide substrates,[10,17,18] which is differently located with respect to the layer perturbed by the electric field in back- and top-gated FEDs (see Fig. 1). In the back-gated geometry, the electric field primarily acts on the buried dead layer, a mixture of conductive and insulating grains[20] where the conducting and magnetic properties are already deteriorated. Hence we do not expect any relevant effect on T_C, whose value is primarily determined by the residual ferromagnetic region near the surface, which could be affected by the applied field only if its penetration depth, or average screening length, was larger than 3 nm. Our data clearly show that this is not the case, in agreement with values for manganite screening lengths reported in literature.[10] On the contrary, the top-gated geometry is expected to be more suitable for inducing field effects on the manganite, in fact the electric field is acting directly on the top ferromagnetic active region of LSMO, while the dead layer is on the opposite part of the film. Note that no dead layer is found at the top interface between the LSMO films and the STO barrier epitaxially grown on top.[14] This is coherent with the experimental observation of the field effect shown in Fig. 3(b) for the top-gated configuration.

With a simple electrostatic model, we can estimate the charge induced per unit surface (σ) in the LSMO layer upon application of the electric field[21]

$$\sigma = \frac{\varepsilon_0 \Delta V}{\delta_{STO}/\varepsilon_{STO} + \lambda_{LSMO}}, \tag{1}$$

where ε_0 and ε_{STO} are the vacuum and static STO permittivities, respectively, δ_{STO} is the insulating barrier thickness, λ_{LSMO} is the LSMO screening length. According to the Thomas–Fermi theory, the induced volume charge density in LSMO decays exponentially moving away from the surface like $\rho_0 \exp(-z/\lambda_{LSMO})$, where z is the distance from the surface and $\rho_0 = \sigma/\lambda_{LSMO}$ is the "surface" modification of the charge density. Assuming $\varepsilon_{STO} = 200$, as obtained from the measurement of the time discharge of the capacitance associated with the FED and in agreement with data reported in literature,[22–25] we find $\rho_0 = 2.45 \times 10^2$ C/cm^3 when 2.5 V are applied. Electrons are then injected in LSMO with a concentration being 1.5×10^{21} cm^{-3} at the interface with STO and $\sim 2 \times 10^{20}$ cm^{-3} one unit cell away from the interface, where the second plane of Mn atoms is placed if we suppose a MnO_2 termination of the LSMO film. For optimally doped LSMO, the carrier density (hole concentration) is about 6×10^{21} cm^{-3}. Assuming that all injected electrons fill holes in Mn^{4+} ions, thus compensating the effect of chemical doping, the application of 2.5 V produces a decrease in the hole doping on the order of 25% and 3.3% on the first and second plane of Mn atoms, respectively. According to the phase diagram for optimally doped LSMO films reported by Tokura *et al.*,[26] which is strictly valid for thick films, such variation would lead to a reduction of the T_C by 25 K considering the charge perturbation on the first MnO_2 layer and only by a few Kelvin moving just to the second layer. This simplified analysis is then in fair agreement with the experimental variation (~5 K), considering that MOKE experiments make an average on the entire LSMO film.

Finally we note that reasonable values for the perturbation of the surface manganite doping due to difference in the work function in heterostructures are of the same order of magnitude of those induced in our FEDs. As a matter of fact in the case of Au/LSMO and Au/STO/LSMO structures,[12–14] the difference in work function between gold and LSMO (5.1 eV and 4.7 eV, respectively) could be the origin of a charge transfer giving an interfacial perturbation of the hole doping of about 6% in the case of direct contact between LSMO and Au. The results obtained in our FED structures indicate that charge transfer between metals and manganites during inter-

face formation cannot account for sizable alterations of the electric and magnetic properties like those reported in our previous works, whose origin is instead related to chemical effects like oxygen vacancy creation.

V. CONCLUSIONS

To summarize, we investigated the effects of electric fields on the magnetic properties of ultrathin LSMO films with Curie temperature close to RT. Our results on back-gated FEDs show no magnetoelectric coupling within the limits imposed by electric breakdown of the STO insulating barrier, in agreement with the fact that in this geometry the screening of the applied field takes place within the magnetically and electrically dead layer. On the contrary a small decrease of T_C ($\sim$5 K) has been observed in top gated devices, where the electric field acts on the "good" portion of the LSMO films, compatible with the estimated reduction of the manganite doping arising from charge injection. These results indicate that only minor magnetoelectric effects can be achieved in vertical FEDs employing STO barriers and ultrathin manganite films with T_C near RT.

ACKNOWLEDGMENTS

We acknowledge Marco Leone for his skilful technical assistance, R. De Renzi, F. Ciccacci, M. Finazzi for fruitful discussions, Xavier Marti for XRD measurements and Maria Varela for and STEM measurements.

[1]H. Béa, M. Gajek, M. Bibes, and A. Barthélémy, J. Phys.: Condens. Matter **20**, 434221 (2008).
[2]H. Béa, M. Bibes, G. Herranz, X.-H- Zhu, S. Fusil, K. Bouzehouane, E. Jacquet, C. Deranlot, and A. Barthélémy, IEEE Trans. Magn. **44**, 1941 (2008).
[3]For a review, see C. H. Ahn, A. Bhattacharya, M. Di Ventra, J. N. Eckstein, C. D. Frisbie, M. E. Gershenson, A. M. Goldman, I. H. Inoue, J. Mannhart, A. J. Millis, A. F. Morpurgo, D. Natelson, and J.-M. Triscone, Rev. Mod. Phys. **78**, 1185 (2006).
[4]W. Eerenstein, M. Wiora, J. L. Prieto, J. F. Scott, and N. D. Mathur, Nature Mater. **6**, 348 (2007).
[5]F. Tsui, M. C. Smoak, T. K. Nath, and C. B. Eom, Appl. Phys. Lett. **76**, 2421 (2000).
[6]R. K. Zheng, Y. Wang, H. L. Chan, C. L. Choy, and H. S. Luo, Phys. Rev. B **75**, 212102 (2007).
[7]A. J. Millis, T. Darling, and A. Migliori, J. Appl. Phys. **83**, 1588 (1998).
[8]Z. G. Sheng, J. Gao, and Y. P. Sun, Phys. Rev. B **79**, 174437 (2009).
[9]H. J. A. Molegraaf, J. Hoffman, C. F. Vaz, S. Gariglio, D. van der Marel, C. H. Ahn, and J.-M. Triscone, Adv. Mater. **21**, 3470 (2009).
[10]X. Hong, A. Posadas, and C. H. Ahn, Appl. Phys. Lett. **86**, 142501 (2005).
[11]I. Pallecchi, L. Pellegrino, E. Bellingeri, A. S. Siri, and D. Marré, Phys. Rev. B **78**, 024411 (2008).
[12]R. Bertacco, S. Brivio, M. Cantoni, A. Cattoni, D. Petti, M. Finazzi, F. Ciccacci, A. A. Sidorenko, M. Ghidini, G. Allodi, and R. De Renzi, Appl. Phys. Lett. **91**, 102506 (2007).
[13]S. Brivio, M. Cantoni, D. Petti, A. Cattoni, R. Bertacco, M. Finazzi, F. Ciccacci, A. A. Sidorenko, G. Allodi, M. Ghidini, and R. De Renzi, Mater. Sci. Eng., B **144**, 93 (2007).
[14]S. Brivio, C. Magen, A. A. Sidorenko, D. Petti, M. Cantoni, M. Finazzi, F. Ciccacci, R. De Renzi, M. Varela, S. Picozzi, and R. Bertacco, Phys. Rev. B **81**, 094410 (2010).
[15]R. Bertacco, M. Cantoni, M. Riva, A. Tagliaferri, and F. Ciccacci, Appl. Surf. Sci. **252**, 1754 (2005).
[16]By courtesy of M. Varela and C. Magen, Oak Ridge National Laboratory, Oak Ridge, Tennessee 37831, USA.
[17]J. Z. Sun, D. W. Abraham, R. A. Rao, and C. B. Eom, Appl. Phys. Lett. **74**, 3017 (1999); A. A. Sidorenko, G. Allodi, R. De Renzi, G. Balestrino, and M. Angeloni, Phys. Rev. B **73**, 054406 (2006); J.-H. Liao, Y.-S. Lo, and T.-B. Wu, J. Cryst. Growth **310**, 3861 (2008); K. Yoshimatsu, K. Horiba, H. Kumigashira, E. Ikenaga, and M. Oshima, Appl. Phys. Lett. **94**, 071901 (2009).
[18]M. Huijben, L. W. Martin, Y.-H. Chu, M. B. Holcomb, P. Yu, G. Rijnders, D. H. A. Blank, and R. Ramesh, Phys. Rev. B **78**, 094413 (2008).
[19]K. Szot, W. Speier, G. Bihlmayer, and R. Waser, Nature Mater. **5**, 312 (2006).
[20]E. Dagotto, T. Hotta, and A. Moreo, Phys. Rep. **344**, 1 (2001).
[21]M. Y. Zhuravlev, R. F. Sabirianov, S. S. Jaswal, and E. Y. Tsymbal, Phys. Rev. Lett. **94**, 246802 (2005).
[22]H.-C. Li, W. Si, A. D. West, and X. X. Xi, Appl. Phys. Lett. **73**, 464 (1998).
[23]J. P. Hong, J. S. Kwak, C. O. Kim, S. J. Park, J. H. Sok, and E. H. Lee, J. Appl. Phys. **88**, 3592 (2000).
[24]H.-M. Christen, J. Manhart, E. J. Williams, and C. Gerber, Phys. Rev. B **49**, 12095 (1994).
[25]J. H. Hao, Z. Luo, and J. Gao, J. Appl. Phys. **100**, 114107 (2006).
[26]Y. Tokura, Y. Tomioka, H. Kuwahara, A. Asamitsu, Y. Morimoto, and M. Kasai, J. Appl. Phys. **79**, 5288 (1996).